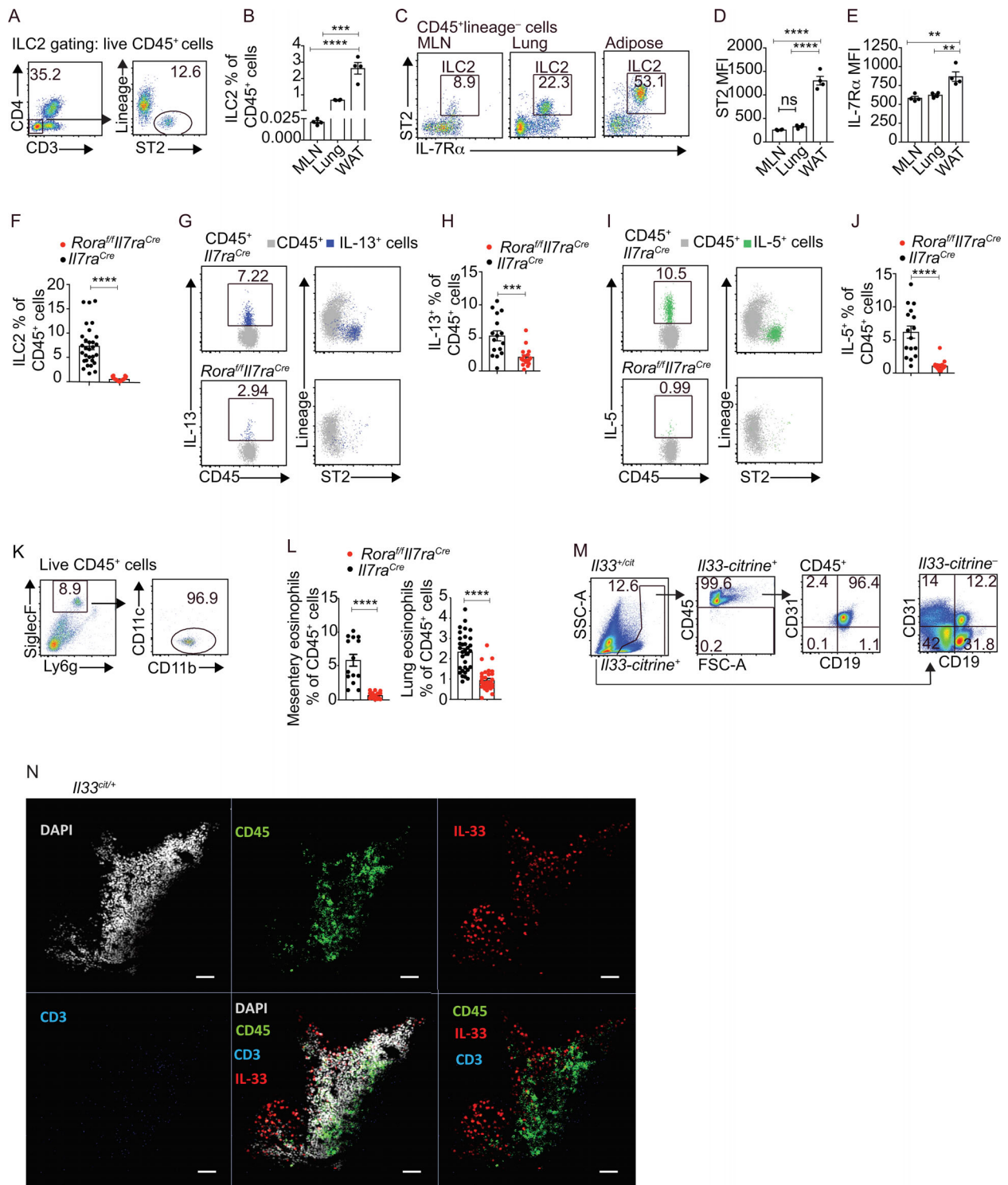


## Supplemental material

Rana et al., <https://doi.org/10.1084/jem.20190689>



**Figure S1. Characterization of ILC2s and MSCs in WAT.** (A) Gating strategy for lineage<sup>-</sup>ST2<sup>+</sup> ILC2s. (B and C) Flow cytometric analysis of Lin<sup>-</sup>IL-7R $\alpha$ <sup>+</sup>ST2<sup>+</sup> ILC2 populations in the MLN, lung, and WAT ( $n = 4$ ). (D and E) ST2 (D) and IL-7R $\alpha$  (MFI; E) expression by Lin<sup>-</sup>IL-7R $\alpha$ <sup>+</sup>ST2<sup>+</sup> ILC2s harvested from the MLN, lung, and WAT ( $n = 4$ ). (F) ILC2 frequency in the mesentery of control (*Il7ra*<sup>Cre</sup>) and ILC2-deficient (*Rora*<sup>fl/fl</sup>*Il7ra*<sup>Cre</sup>) mice. Data are pooled from four independent experiments ( $n = 33$  and 35). (G and H) Intracellular flow cytometric analysis showing a representative example of IL-13<sup>+</sup>CD45<sup>+</sup> populations (G) and as a percentage of total CD45<sup>+</sup> cells in the mesentery of (*Il7ra*<sup>Cre</sup>) and ILC2-deficient (*Rora*<sup>fl/fl</sup>*Il7ra*<sup>Cre</sup>) mice (H). Data are pooled from two independent experiments ( $n = 15$ –17). (I and J) Intracellular flow cytometric analysis showing a representative example of IL-5<sup>+</sup>CD45<sup>+</sup> populations (I) and as a percentage of total CD45<sup>+</sup> cells in the mesentery of (*Il7ra*<sup>Cre</sup>) and ILC2-deficient (*Rora*<sup>fl/fl</sup>*Il7ra*<sup>Cre</sup>) mice (J). Data are pooled from two independent experiments ( $n = 15$ –17 mice). (K) Gating strategy for eosinophils. (L) Eosinophil frequency in control (*Il7ra*<sup>Cre</sup>) and ILC2-deficient (*Rora*<sup>fl/fl</sup>*Il7ra*<sup>Cre</sup>) mice. Data are pooled from two independent experiments ( $n = 15$ –17). (M) Phenotyping of *Il33*-citricine<sup>+</sup> cells in bone marrow. Representative data ( $n = 4$  mice). (N) Histology of fat associated lymphoid clusters in the perigonadal fat from WT mice. Scale bars, 50  $\mu$ m. Data are represented as mean  $\pm$  SEM. \*\*,  $P < 0.01$ ; \*\*\*,  $P < 0.001$ ; \*\*\*\*,  $P < 0.0001$ ; one-way ANOVA with Tukey's post hoc test (B, D, and E), or Student's  $t$  test (F, H, J, and L).

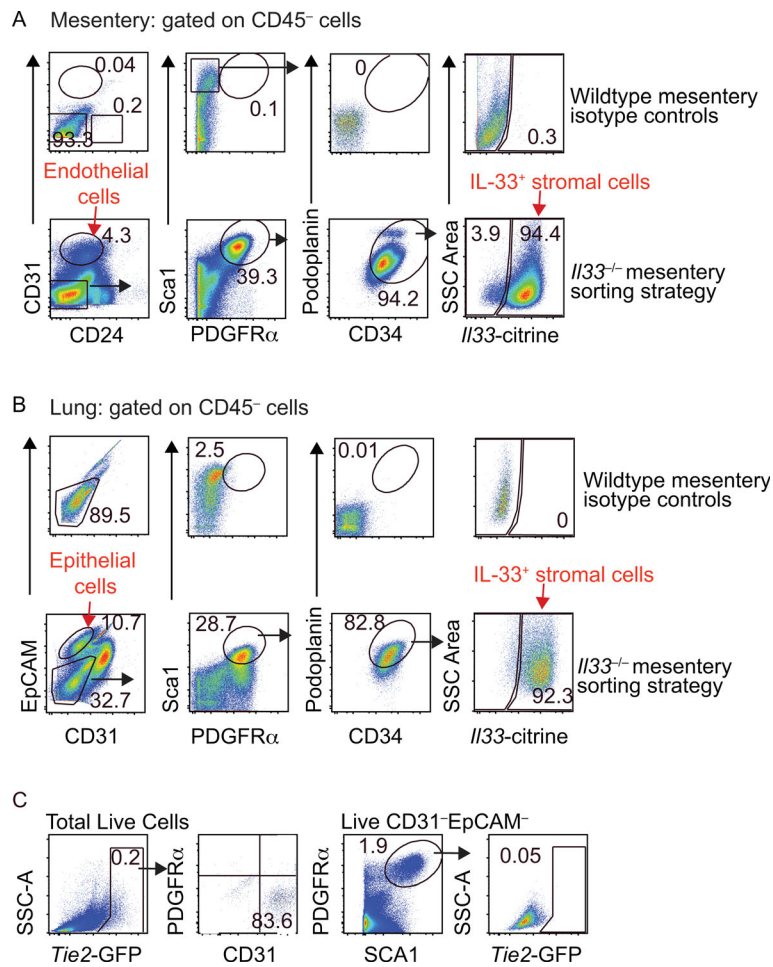


Figure S2. **Gating strategies. (A and B)** Gating strategy used to purify cell populations for RNA-seq analysis. **(C)** Flow cytometric analysis of *Tie2*-GFP<sup>+</sup> mesentery. *Tie2*-GFP gate was determined based on WT mice (representative of two mice).

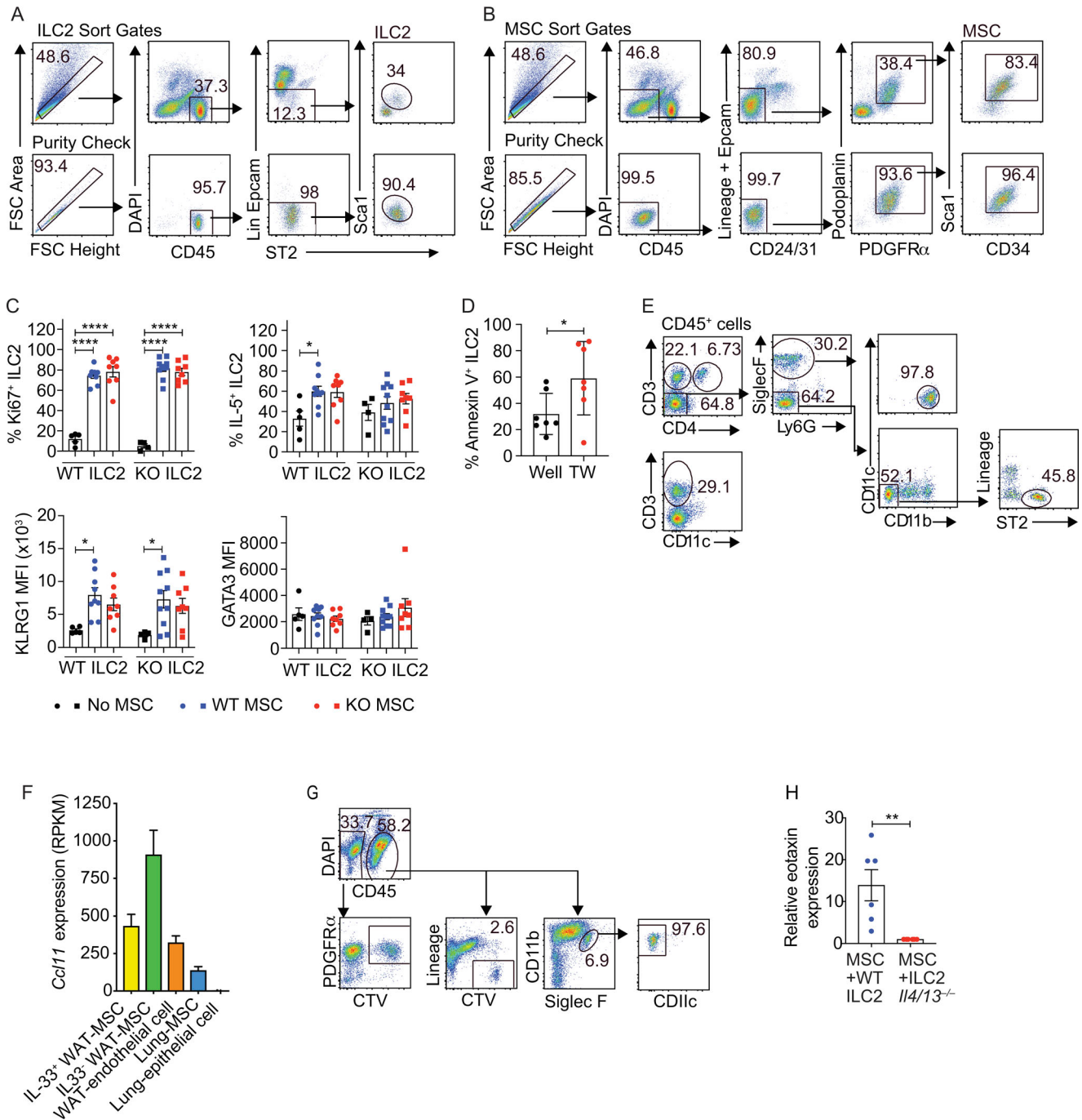


Figure S3. **Gating strategies and schematic of cross-talk between MSCs, ILC2, and eosinophils. (A and B)** Flow cytometry gating strategy and purity check for WAT-ILC2s and WAT-MSCs. **(C)** Proportion of Ki67<sup>+</sup>ILC2, IL5<sup>+</sup>ILC2, KLRG1 MFI, and GATA3 MFI from co-cultured WT or *Il33*<sup>-/-</sup> (KO) ILC2 and WT or *Il33*<sup>-/-</sup> WAT-MSCs, after 7 d. Cumulative data pooled from three independent experiments (*n* = 4–10). Cumulative data pooled from three independent experiments (*n* = 4–10). **(D)** Cell death of ILC2 determined on TW substrate or tissue culture plate surface by annexin V staining. Pooled data from two experiments (*n* = 7). **(E)** Gating strategy for T cells, eosinophils, and ILC2s. **(F)** *Ccl11* gene expression (reads per kilobase of transcript per million mapped reads; RPKM) in the tissues indicated (*n* = 3). **(G)** Gating strategy for CTV<sup>+</sup>WAT-MSCs, CTV<sup>+</sup>ILC2s and eosinophils in Matrigel plugs. **(H)** Relative eotaxin expression in supernatants from MSCs and ILC2 (WT, BALB/c WT, or BALB/c *Il4*<sup>-/-</sup>/*Il13*<sup>-/-</sup>) co-cultured overnight. Pooled data from six experiments. Mann–Whitney *U* test. Data are represented as mean  $\pm$  SEM. \*, *P* < 0.05; \*\*, *P* < 0.01; \*\*\*\*, *P* < 0.0001.